GSA Data Repository 2015310

Supplemental Material to the Manuscript "The impact of dynamic topography change on Antarctic ice sheet stability during the mid-Pliocene warm period"

by J. Austermann, D. Pollard, J.X. Mitrovica, R. Moucha, A.M. Forte, R.M. DeConto, D.B. Rowley, and M.E. Raymo

I. Methodology

We use the numerical code ASPECT (aspect.dealii.org; Kronbichler et al., 2012) to simulate compressible convective flow in the Earth's mantle. As input, we adopt the density model TX2008 that has been derived on the basis of a joint inversion of a large database of shear-wave travel times and geodynamic data, with a scaling between seismic wave speeds and density based on constraints from mineral physics (Simmons et al., 2009). The geodynamic data include present-day observables such as long-wavelength free-air gravity anomalies, residual topography, plate divergence, and excess ellipticity of the core-mantle boundary. We further use a 3-D viscosity field that is based on the radial model V2 (Fig. DR1). This radial profile was derived from a joint inversion of the geodynamic data set and a suite of observables related to glacial isostatic adjustment (Mitrovica and Forte, 2004; Forte et al., 2010). The simulations do not incorporate mantle phase changes, and we therefore assume adiabatic density and temperature profiles across the mantle. In order to produce realistic mantle temperatures, the top surface of the model domain is set to 1600 K and the core-mantle boundary temperature is then (following the assumption of adiabaticity) 2400 K, neglecting thermal boundary layers. The depth-varying thermal conductivity, thermal expansivity and heat capacity are adopted from Glisovic et al. (2014). ASPECT does not calculate gravity self consistently and we impose the radially varying gravity profile from Glisovic et al. (2014). We do not include internal heating from radioactive decay in the flow simulations.

We apply a free slip boundary condition at the core-mantle boundary and a no slip boundary condition at the top surface. Since the Antarctic plate is relatively stationary, this approach yields results comparable to those obtained by applying present-day plate velocities as a boundary condition on the top surface. The depth resolution of our numerical grid is ~60km in the upper 1000km and varies from 130km to 230km below this depth. The lateral resolution is on the order of 140km in the upper 1000km and 350km to 500km below this depth. The timesteps are of order 50 kyr, as derived from a Courant-Friedrichs-Lewy (CFL) number of 0.2. We run ASPECT forward in time to calculate the rate of change of dynamic topography and have confirmed that the solution converges for the adopted tolerance of the linear solver and the spatial resolution. The dynamic topography change is then extrapolated back to 3 Ma. To calculate dynamic topography from the radial stresses of the mantle convection model we incorporate gravitationally self-consistent sea level variations driven by the effects of dynamic topography and associated ocean load changes (Austermann and Mitrovica, 2015).

As a first benchmarking exercise, we compared results from an ASPECT simulation using the 1-D viscosity profile V2 (i.e., no lateral variations in viscosity are imposed) to predictions from a global convection model used in Rowley et al. (2013) that are based on a spectral solution of the governing field equations (Forte and Peltier, 1991, 1994) and the same density and (radially varying) viscosity fields. There are several differences in the two approaches. Specifically, Rowley et al. (2013) use a distinct formulation of the top boundary condition (Forte and Peltier, 1994), a different spatial resolution, a self-consistent treatment of gravity, and a backward advection scheme for computing the change in dynamic topography since 3 Ma. Figure DR2 presents a comparison of the dynamic topography change over Antarctica computed using the two approaches. The agreement is satisfactory.

In the calculations described in the main text, we incorporate lateral variations in mantle viscosity linked to temperature perturbations. The three-dimensional viscosity field is calculated from the expression:

$$\eta(\varphi,\theta,r) = \eta_0(r)\cdot\exp(-\varepsilon\cdot(T(\varphi,\theta,r)-T_0(r)))$$

where η_0 is the depth varying viscosity profile V2, T_0 is the adiabatic temperature profile and ε is an activation parameter (Ratcliff et al., 1996; Zhong et al., 2000). In the main text, we choose ε to be 0.02; in this case, 70% and 95% of the grid points in the mantle below the Antarctic plate are within ±1 and ±2 orders of magnitude relative to the depth average, respectively.

Figure DR1. Radially varying viscosity profiles V1 and V2 derived from a joint inversion of convection and glacial isostatic adjustment observations (Mitrovica and Forte, 2004; Forte et al., 2010).

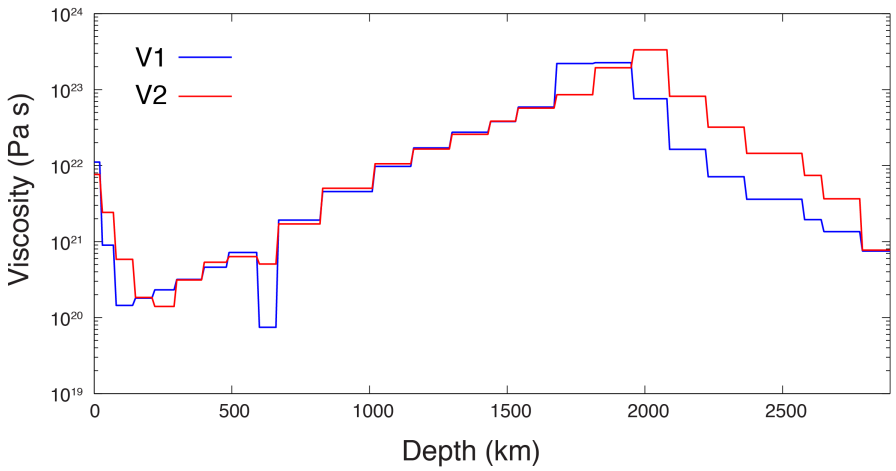

Figure DR2. Computed change in dynamic topography since 3 Ma. (A) Prediction from the Rowley et al. (2013) simulation, and (B) from our calculation using the ASPECT convection code. Both predictions assume a water-loaded dynamic topography, the 1-D viscosity profile V2 and no plate motions.

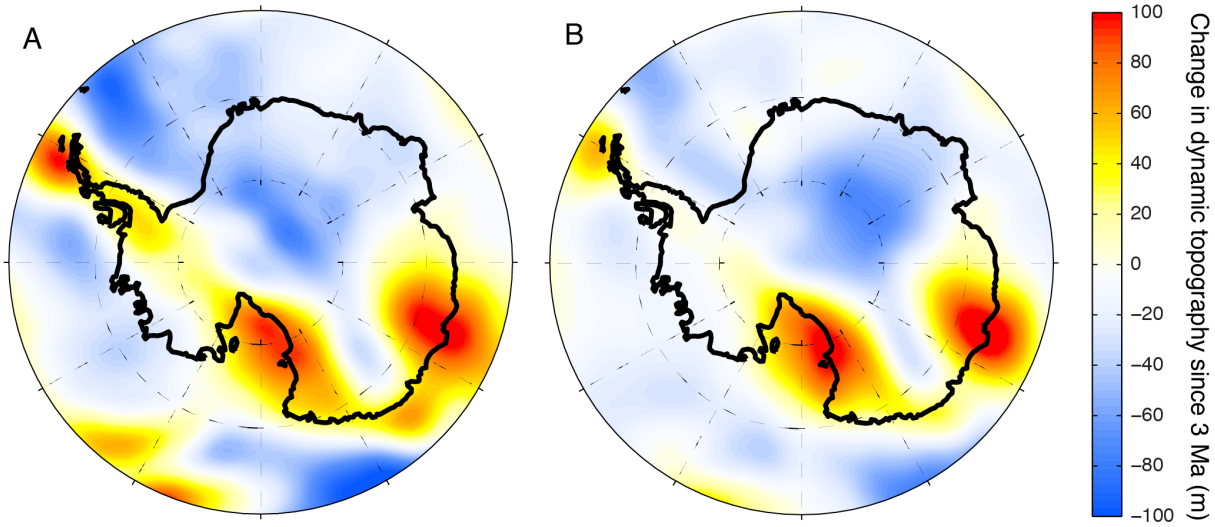

II. Sensitivity studies

Figure DR3. Two vertical cross-sections (see inset for orientation) through three different shear wave tomography models: S40RTS (Ritsema et al., 2011), Savani (Auer et al., 2014) and GyPSuM (Simmons et al., 2010). These models all show a slow shear wave velocity anomaly in the mid mantle below the Transantarctic Mountains (panels A-C, transect a-a'). They also all show a transition from slow upper mantle seismic wave speeds north of the Wilkes Basin to fast wave speeds within the East Antarctic craton (panels D-F, transect b-b'). Note that the variable extent of the East Antarctic craton in sections D-F will impact the location of the predicted corner flow upwelling at the northern edge of the Wilkes Basin.

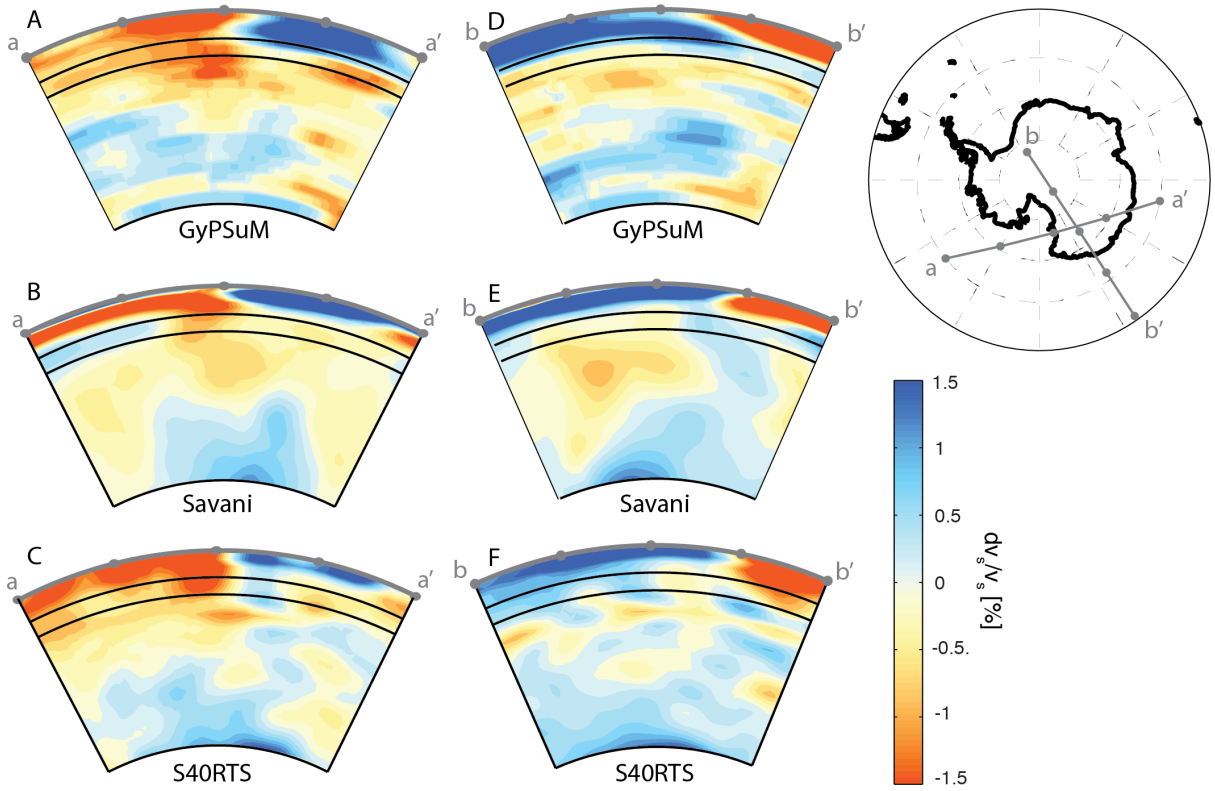

Figure DR4. Sensitivity of dynamic topography predictions to various input parameters. The prediction discussed in the main text is based on the tomography model TX2008, the radial viscosity profile V2, lateral variations in viscosity prescribed using ε = 0.02 (see section I of this supplement), and the plate reference frame of Sella et al. (2002). The following frames show predictions of dynamic topography in which these input parameters are varied. Specifically: A) smaller lateral variations in viscosity (ε = 0.01); B) radial viscosity profile V1 (see Fig. DR1); C) plate velocity reference frame from Quéré et al. (2007); D) plate velocity reference Müller et al. (1993); E) same as D, but with ε = 0.01; and F) plate velocity reference frame from Doubrovine et al. (2012). In each case, the white arrow indicates the Antarctic plate velocity relative to the model domain. Predictions of Pliocene ice sheet extent based upon these computed changes in dynamic topography are shown in Figure DR5. Note that estimates of the Antarctic plate motion based on hotspot reference frames vary from one another (Müller et al., 1993; Gripp and Gordon, 2002; Doubrovine et al., 2012), while present-day motions based on geodetic measurements and a no-net-rotation reference frame are relatively consistent (Larson et al., 1997; Sella et al., 2002; Jiang et al., 2009). The Antarctic plate is surrounded by oceanic ridges and is therefore relatively stationary.

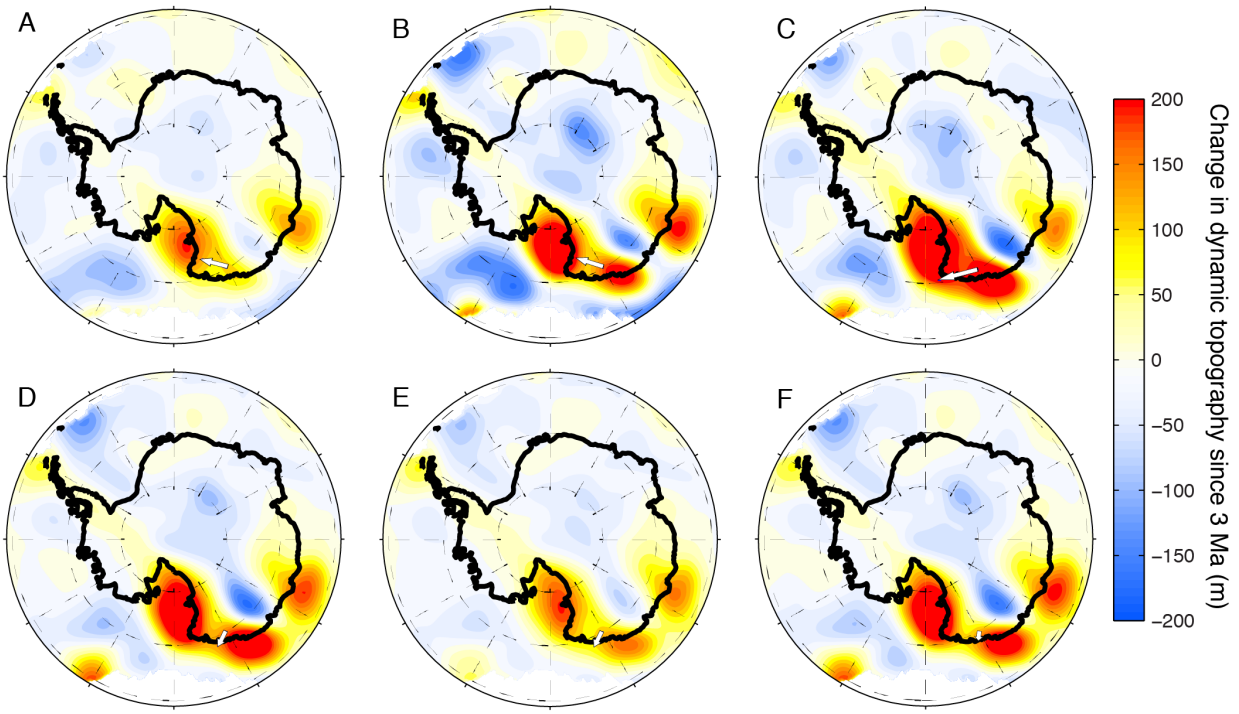

Figure DR5: Sensitivity of our simulation of ice sheet extent at 3 Ma to different predictions of the change in dynamic topography within a region in the vicinity of the Wilkes Basin. Panels A-F are ice sheet simulations associated with the dynamic topography changes shown in panels A-F of Figure DR4. The predicted shoreline retreat in the Wilkes Basin, relative to an ice sheet simulation with no change in dynamic topography, is approximately 200km (A), 480km (B), 560km (C), 430km (D), 300km (E), and 250km (F). The difference in predicted ice volume relative to the simulation without dynamic topography is, in units of equivalent globally averaged sea-level change, 1.3m (A), 2.3m (B), 2.8m (C), 2.1m (D), 1.1m (E), and 1.6m (F).

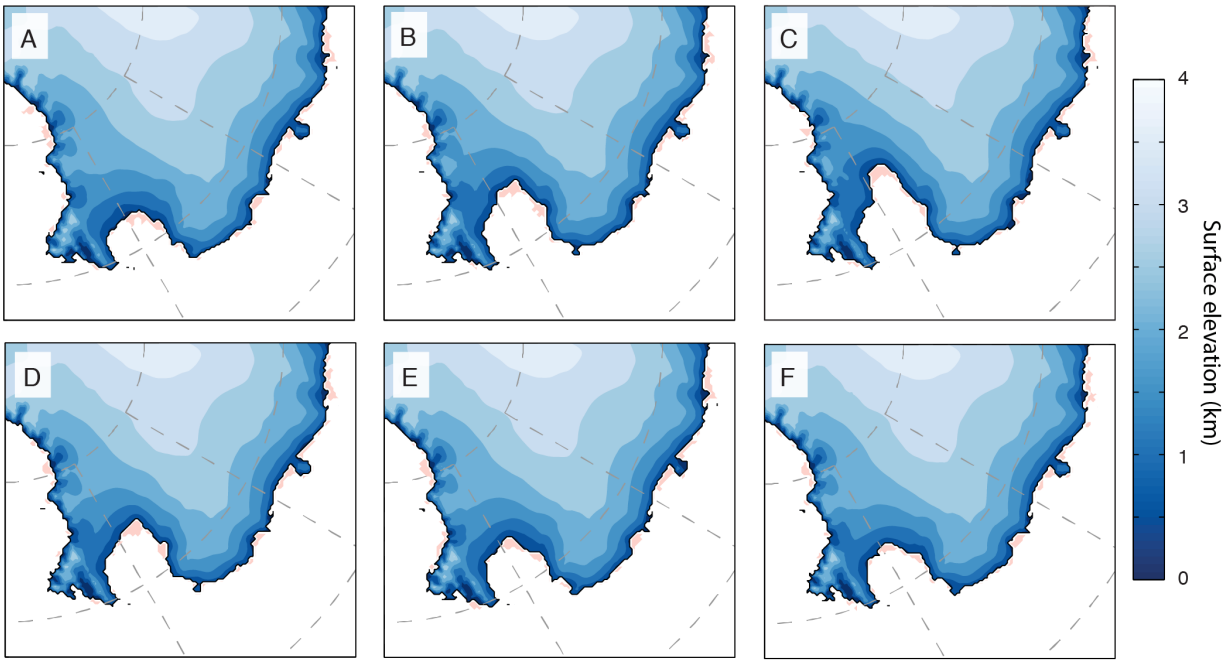

Figure DR6: Ice sheet model predictions under MPWP conditions without (A and B) and with (C and D) dynamic topography. Frames A and C are reproduced from Figure 3A and 3B of the main text. Frames B and D are simulations identical to A and C, respectively, except that the ice models include the additional instability mechanisms of cliff failure at ice margins and hydrofracturing (Pollard et al., 2015).

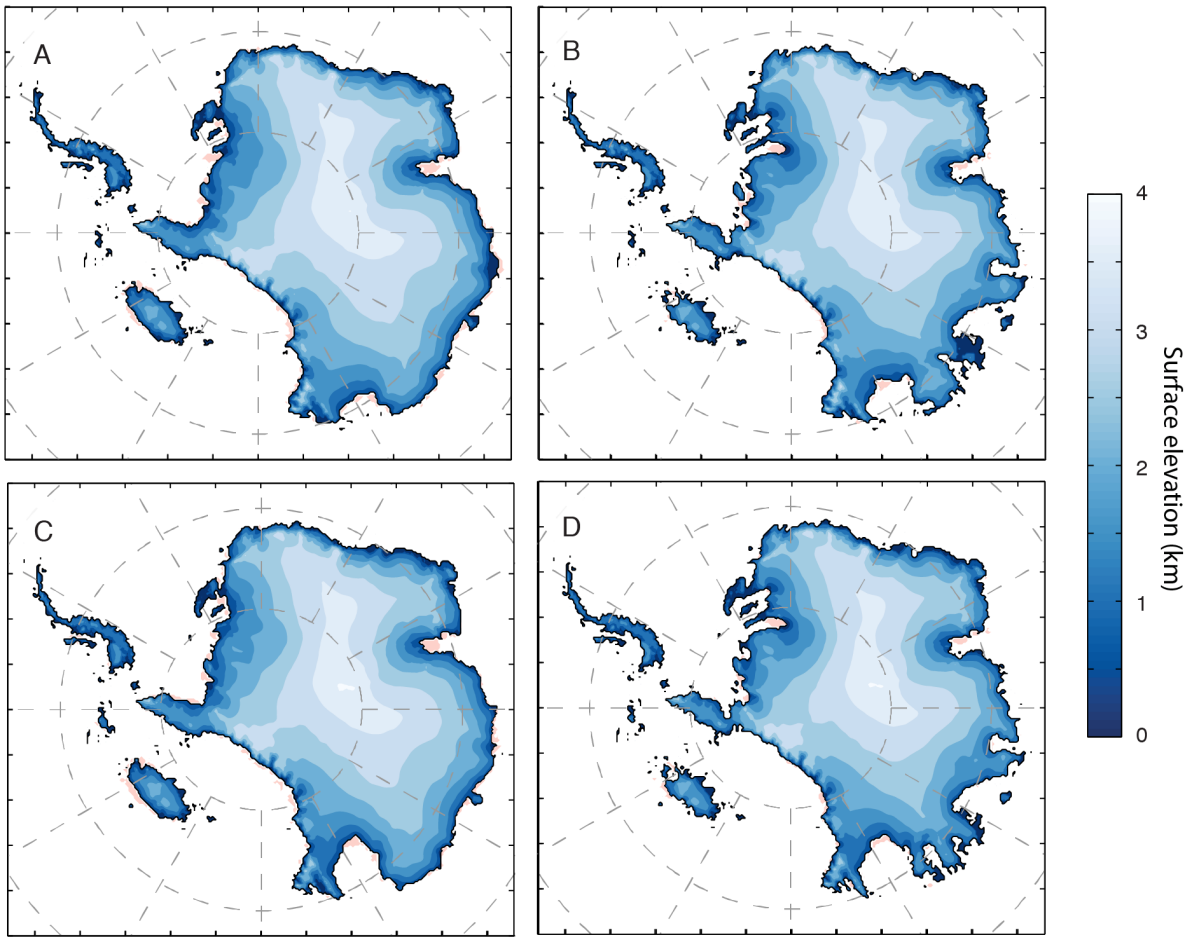

References cited in the supplement

Auer, L., Boschi, L., Becker, T.W., Nissen-Meyer, and T., Giardini, D., 2014, Savani: A variable resolution whole-mantle model of anisotropic shear velocity variations based on multiple data sets, J. Geophys. Res. doi:10.1002/2013JB010773.

Austermann, J., and Mitrovica, J.X., 2015, Calculating gravitationally self-consistent sea level changes driven by dynamic topography, 2015, Geophys. J. Int., in review.

Doubrovine, P.V., Steinberger, B., and Torsvik, T.H., 2012, Absolute plate motions in a reference frame defined by moving hot spots in the Pacific, Atlantic, and Indian oceans, J. Geophys. Res. 117, B09101.

Forte, A. M., and Peltier, W.R., 1991, Viscous flow models of global geophysical observables: 1. Forward problems, J. Geophys. Res. 96, p. 20,131–20,159.

Forte, A.M., and Peltier, W.R., 1994, The kinematics and dynamics of poloidal–toroidal coupling in mantle flow: The importance of surface plates and lateral viscosity variations, Adv. Geophys. 36, p. 1–119.

Forte, A.M., Quéré, S., Moucha, R., Simmons, N.A., Grand, S.P., Mitrovica, J.X., and Rowley, D.B., 2010, Joint seismic-geodynamic-mineral physical modelling of African geodynamics: A reconciliation of deep-mantle convection with surface geophysical constraints, Earth Planet. Sci. Lett. 295, 329 – 341.

Gripp, A.E., and Gordon, R.G., 2002, Young tracks of hotspot and current plate velocities, Geophys. J. Int. 150, p. 321-361.

Glisovic P., and Forte, A.M., 2014, Importance of initial buoyancy field on evolution of mantle thermal structure: Implications of surface boundary conditions, Geosc. Front. 6(1), 3-22.

Jiang, W.-P., E, D.-C., Zhan, B.-W., and Liu, Y.-W., 2009, New model of Antarctic plate motion and its analysis, Chinese J. Geophys. 52, p. 23-32.

Kronbichler, M., Heister, T., and Bangerth, W., 2012, High accuracy mantle convection simulation through modern numerical methods, Geophys. J. Int. 191, p. 12-29.

Larson, K.R., Freymueller, J.T., and Philipsen, S., 1997, Global plate velocities from the Global Positioning System, J. Geophys. Res. 102, p. 9961-9981.

Mitrovica, J.X., and Forte, A.M., 2004, A new inference of mantle viscosity based upon joint inversion of convection and glacial isostatic adjustment data, Earth Planet. Sci. Lett. 225, p. 177-189.

Müller, R.D., Royer, J.-Y. and Lawver, L.A., 1993, Revised plate motions relative to the hotspots from combined Atlantic and Indian Ocean hotspot tracks, Geology 21, p. 275-278.

Pollard, D., DeConto, R.M., and Alley, R.B., 2015, Potential Antarctic Ice Sheet retreat driven by hydrofracturing and ice cliff failure, Earth Planet. Sci. Lett. 412, p. 112-121.

Ratcliff, J.T., Schubert, G., and Zebib, A., 1996, Effects of temperature-dependent viscosity on thermal convection in a spherical shell, Physica D 97, p. 242-252.

Ritsema, J., Deuss, A., van Heijst, H.J., and Woodhouse, J.H., 2011, S40RTS: a degree-40 shear-velocity model for the mantle from new Rayleigh wave dispersion, teleseismic traveltime

and normal-mode splitting function measurements, Geophys. J. Int. 184, 1223-1236.
Rowley, D.B., Forte, A.M., Moucha, R., Mitrovica, J.X., Simmons, N.A., and Grand, S.P., 2013, Dynamic Topography Change of the Eastern United States Since 3 Million Years Ago, Science 340, p. 1560-1563.
Sella, G., Dixon, T.H., and Mao, A., 2002, REVEL: A model for recent plate velocities from space geodesy, J. Geophys. Res. 107, ETG 11-1 – 11-30.
Simmons, N.A., Forte, A.M., and Grand, S.P., 2009, Joint seismic, geodynamic and mineral physical constraints on three-dimensional mantle heterogeneity: Implications for the relative importance of thermal versus compositional heterogeneity, Geophys. J. Int. 117, p. 1284-1304.
Simmons, N.A., Forte, A.M., Boschi, and L., Grand, S.P., 2010, GyPSuM: A joint tomographic model of mantle density and seismic wave speeds, J. Geophys. Res. 115, B12310.
Quéré, S., Rowley, D.B., Forte, A.M., and Moucha, R., 2007, No-net-rotation and Indo-Atlantic hotspot reference frames: towards a new view of tectonic plate motions and Earth dynamics, Fall Meet. Suppl., Abstract U34A-03. Eos Trans. AGU, vol. 88.
Zhong, S., Zuber, M.T., Moresi, L., and Gurnis, M., 2000, Role of temperature-dependent viscosity and surface plates in spherical shell models of mantle convection, J. Geophys. Res. 105 (B5), p. 11,063-11,082.